Passively Mode-Locked 4.6 and 10.5 GHz Quantum Dot Laser Diodes Around 1.55 μm With Large Operating Regime

Martijn J. R. Heck, *Member, IEEE*, Amandine Renault, Erwin A. J. M. Bente, *Member, IEEE*, Yok-Siang Oei, Meint K. Smit, *Fellow, IEEE*, Kjeld S. E. Eikema, Wim Ubachs, Sanguan Anantathanasarn, and Richard Nötzel

Abstract—**Passive mode-locking in two-section InAs/InP quantum dot laser diodes operating at wavelengths around 1.55 μm is reported. For a 4.6-GHz laser, a large operating regime of stable mode-locking, with RF-peak heights of over 40 dB, is found for injection currents of 750 mA up to 1.0 A and for values of the absorber bias voltage of 0 V down to −3 V. Optical output spectra are broad, with a bandwidth of 6–7 nm. However, power exchange between different spectral components of the laser output leads to a relatively large phase jitter, resulting in a total timing jitter of around 35 ps. In a 4-mm-long, 10.5-GHz laser, it is shown that the operating regime of stable mode-locking is limited by the appearance of quantum dot excited state lasing, since higher injection current densities are necessary for these shorter lasers. The output pulses are stretched in time and heavily up-chirped with a value of 16–20 ps/nm. This mode of operation can be compared to Fourier domain mode-locking. The lasers have been realized using a fabrication technology that is compatible with further photonic integration. This makes such lasers promising candidates for, e.g., a coherent multiwavelength source in a complex photonic chip.**

Index Terms—**Mode-locked lasers, quantum dots, semiconductor lasers.**

I. INTRODUCTION

ACTIVE and passive mode-locking of laser diodes is a well-established technique for generating picosecond pulses at wavelengths around 1.55 μm. These wavelengths are of primary interest for telecommunication applications. Mode-locked laser diodes (MLLDs) can be used as high-speed sources in, e.g., optical time-domain multiplexed (OTDM) and wavelength-division multiplexed (WDM) systems [1]. Current interest in

M. J. R. Heck was with the Communication Technology: Basic Research and Applications (COBRA) Research Institute, Eindhoven University of Technology, Eindhoven 5600 MB, The Netherlands, and also with the Laser Centre Vrije Universiteit, Amsterdam 1081 HV, The Netherlands. He is now with the Department of Electrical and Computer Engineering, University of California Santa Barbara, Santa Barbara, CA 93106 USA (e-mail: mheck@ece.ucsb.edu).

A. Renault was with the Laser Centre Vrije Universiteit, Amsterdam 1081 HV, The Netherlands. She is now with ASML, Veldhoven 5504 DR, The Netherlands (e-mail: amandine.renault@asml.com).

E. A. J. M. Bente, Y.-S. Oei, M. K. Smit, S. Anantathanasarn, and R. Nötzel are with the COBRA Research Institute, Eindhoven University of Technology, Eindhoven 5600 MB, The Netherlands (e-mail: e.a.j.m.bente@tue.nl; s.anantathanasarn@tue.nl; r.noetzel@tue.nl; y.s.oei@tue.nl; m.k.smit@tue.nl).

K. S. E. Eikema and W. Ubachs are with the Laser Centre Vrije Universiteit, Amsterdam 1081 HV, The Netherlands (e-mail: kse.eikema@few.vu.nl; wimu@few.vu.nl).

Digital Object Identifier 10.1109/JSTQE.2009.2016760

these MLLDs lies in utilizing the coherent bandwidth that these lasers generate in combination with mature optical fiber-based technology in advanced optical (telecommunication) systems, such as optical code-division multiple-access (O-CDMA) systems [2], arbitrary waveform generation [3], clock distribution and as multiwavelength sources for silicon-based integrated optics [4], [5]. Moreover, these MLLDs have found their way to other fields of research, such as biomedical imaging [6] and frequency comb generation [7], e.g., for metrology purposes.

The material typically used for fabricating these MLLDs operating at 1.55 μm is InP/InGaAsP, using either bulk or quantum-well gain sections [8]. In recent years, however, quantum dot (QD) gain material has been shown to be promising for application in MLLDs due to the broad gain spectrum, low spontaneous emission levels, reduced linewidth enhancement factor, and a low threshold current density [9], [10]. Also lower sensitivity to optical feedback is reported. Subpicosecond pulse generation with high peak power [11], [12] and low-timing-jitter operation [13] has been achieved. An added advantage is that QD gain material does not suffer from ridge sidewall surface recombination, due to the spatial confinement of the carriers in the dots. As a result, it is possible to make high-contrast ridge waveguides, reducing the size of the devices and increasing the possible integration density [14].

Many of these advantages have been reported with two-section MLLDs based on InGaAs/GaAs QD gain material, which operate in the 1.2–1.3-μm wavelength region. Results obtained with InAs/InP QD or quantum dash material in the 1.5 μm region are scarcer but do already indicate different behavior. Subpicosecond pulse generation [15], [16], and narrow RF linewidths [15], [17] have been observed in MLLDs consisting of only a single section. We have previously reported our first results obtained with monolithic two-section QD lasers based on InAs/InP QD gain material [18], where we have shown that the output pulses are very elongated with a chirp of around 20 ps/nm [19]. This result is strikingly different from what is commonly observed in MLLDs. The observed mode of operation of the laser can be compared to Fourier domain mode-locking [20].

In this paper, which is complementary to the time-domain analysis we have presented in [19], the operating regime for stable mode-locking of InAs/InP QD MLLDs is explored, and the boundaries of this stability regime are studied. We will show that these lasers have much larger ranges for the optical amplifier current and saturable absorber voltages for passively mode-locked

operation compared to quantum well or bulk lasers, based on the InP/InGaAsP material and operating around 1.55 μm. Having a large and robust stability regime is essential for practical implementation of these lasers as low-cost and stable sources [21]. The characterization results presented in this paper also lead to a better understanding of the operation of these MLLDs and again show the operation to be very different from that of lasers based on InAs/GaAs QDs. In particular, our results show the strong influence of the inhomogeneous character of the QD gain medium and its limitations to stable mode-locking.

In this paper, first the device design and fabrication are presented in Section II. Hereafter, the experimental results are presented and discussed for a laser configuration with a total length of 9 mm (Section III-A). This laser shows the largest stability regime. In Section III-B, we present the results from lasers with a length of 4 mm. Due to their shorter length, higher current densities are required and as a result lasing on the excited state (ES) of the QDs takes place. The effect of this ES-lasing on the stability of mode-locking is discussed. The conclusions are then summarized in Section IV.

II. DESIGN AND FABRICATION

The QD laser structure is grown on n-type (100) InP substrates by metal–organic vapor phase epitaxy (MOVPE), as presented in [14] and [18]. In the active region five InAs QD layers are stacked. These are placed in the center of a 500-nm InGaAsP optical waveguiding core layer. The bottom cladding of this laser structure is a 500-nm-thick n-InP buffer and the top cladding is a 1.5-μm p-InP with a compositionally graded 300-nm p-InGaAs(P) top contact layer. This layerstack is compatible with the butt-joint active–passive integration process as mentioned in [22], [23] for possible further integration.

Two-section Fabry–Pérot-type (FP) laser devices have been designed and realized with total lengths of 4 and 9 mm and section ratios of 3% up to 30%, as shown in Fig. 1(a). The ridge waveguides have a width of 2 μm and are etched approximately 150 nm into the InGaAsP layer [Fig. 1(b)]. To create electrical isolation between the two sections, the most highly doped part of the p-cladding layer is etched away. The waveguide and isolation sections are etched using a CH_4/H_2 two-step reactive-ion dry etch process. The structures are planarized using polyimide. Evaporated and gold-plated metal pads create electrical contacts to both sections. The backside of the n-InP substrate is metalized to act as a common ground contact for the two sections.

The structures are cleaved to create the mirrors of the FP-cavity. No coating is applied. The two-section devices are operated by forward biasing the longer gain section, creating a semiconductor optical amplifier (SOA) and by reversely biasing the shorter gain section, creating a saturable absorber (SA). The devices are mounted on a temperature-controlled copper chuck, p-side up.

III. EXPERIMENTAL RESULTS

In this section, we present the results from a study on passive mode-locking in two sets of lasers with a total length of 9 and 4 mm and corresponding repetition rates of 4.6 and 10 GHz. The
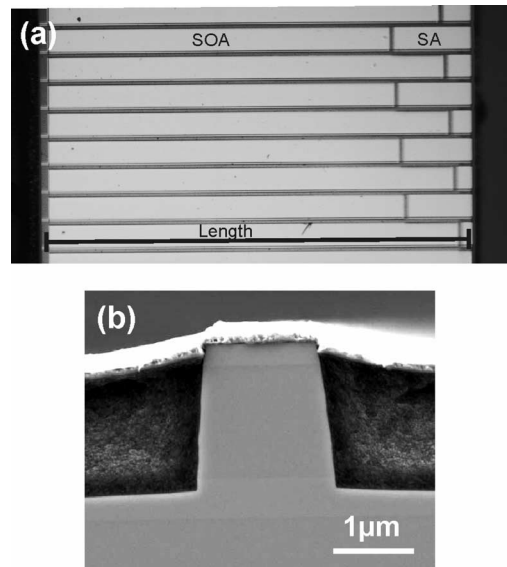

Fig. 1. (a) Photograph of the realized devices, showing different configurations. The SOA (gain) and SA (saturable absorption) sections are indicated. (b) Scanning electron microscope picture of the waveguide cross-section. To facilitate cleaving, gold plating was omitted at the ends of the waveguides and only a 300-nm-thick evaporated metal contact layer is visible in the picture.
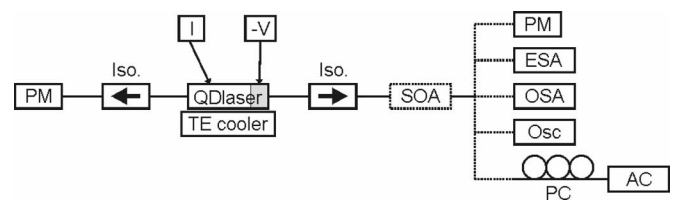

Fig. 2. Schematic overview of the setup used to characterize the QD lasers. PM: power meter, Iso: optical isolator, TE cooler: thermoelectric cooler, SOA: optional booster amplifier, ESA: electrical spectrum analyzer including a 50 GHz photodiode, OSA: optical spectrum analyzer, Osc: 6-GHz real-time oscilloscope including 45 GHz photodiode, PC: polarization controller, AC: autocorrelator. All equipment is fiber pigtailed or has fiber input or output connectors. A current source (I) and voltage source (−V) are used to bias the SOA and SA, respectively.

characterization setup used is depicted in Fig. 2. Antireflection coated lensed fibers are used to collect the laser output and optical isolators are used to prevent feedback from reflections into the laser cavity. The copper chuck below the laser is kept at a fixed temperature of 10 °C. Needle probes are used to bias the two sections of the laser. A commercial SOA is used to optionally boost the optical output power. The SOA is operated at a gain level of 6–7 dB.

A. Passive Mode-Locking in 9 mm MLLDs

In this section, we compare the results obtained with 9mm MLLDs having a 270 and a 540 μm SA. The shortest SA available in our set was 270 μm and the maximum SA length was 540 μm where we observed stable mode-locking. A single-section 9 mm FP-laser, fabricated on the same chip is used for reference purposes, e.g., to compare threshold currents.

The laser with a 270 μm SA section has lasing threshold current values of 660–690 mA for SA reverse bias voltages of
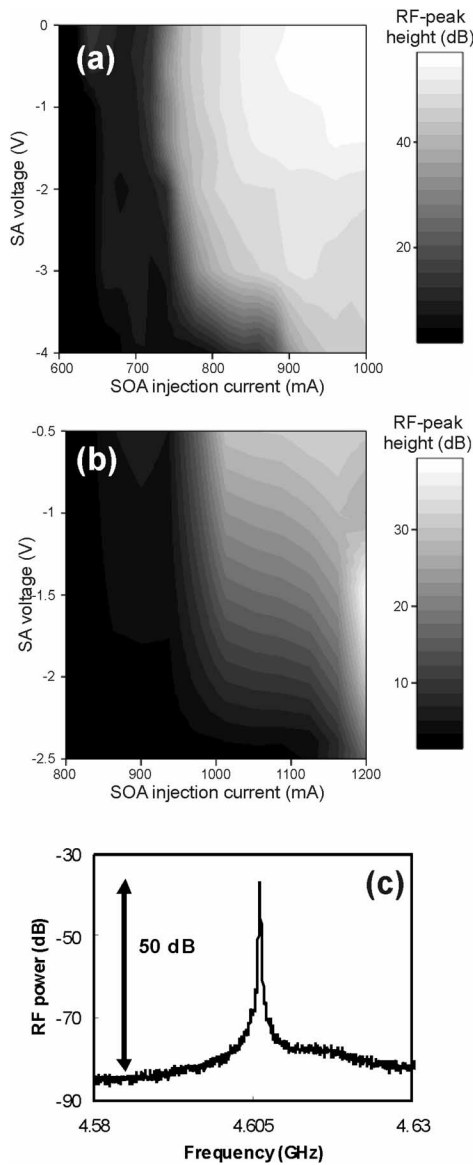
Fig. 3. Height of the peak at the fundamental frequency in the observed electrical RF power spectra from the photodiode [over the noise floor, dB-scale (c)] for a 9 mm laser with (a) a 270 μm SA and (b) a 540 μm SA. The electrical bandwidth used to obtain the RF spectra is 50 kHz. An external SOA was used before the 50 GHz photodiode to boost the optical output power of the 270 μm laser by 6–7 dB. The 540 μm laser was directly connected to the photodiode, without an SOA. The RF power is grayscale coded in dB. An example for an injection current of 900 mA and an SA bias voltage of −1 V is shown in (c).

0 to −4 V, respectively. Passive mode-locking is first studied by recording the electrical power spectrum using a 50-GHz photodiode and a 50-GHz electrical spectrum analyzer (Fig. 2). The RF spectra obtained for this laser show clear peaks at the cavity roundtrip frequency of 4.6 GHz. In Fig. 3, the height of these RF peaks over the noise floor is given as a function of the operation parameters, i.e., the SA bias voltage and the SOA injection current. A large, robust operating regime with RF-peak heights over 40 dB, indicative for stable mode-locking [24], and having optical output powers of 1–4 mW is found for values of the injection current of 750 mA up to 1.0 A and for values of the SA bias voltage of 0 down to −3 V. Within this regime

the width of the RF peak is narrow, i.e., ranging from 0.4 to 0.8 MHz at the −20 dB level for bias voltages of 0 down to −1.5 V. For SA bias voltages of −2 down to −3 V, this width is in the range of 0.8–2.5 MHz. Also the position of this RF peak, which is centered around 4.6 GHz, is stable within 6 MHz for the operating regime mentioned above. In MLLDs, based on bulk gain material minimum RF linewidths of 2.5 MHz at −20 dB have been reported, with a variation of the roundtrip frequency of about 50 MHz over their operating regime [25]. So a clear improvement of the stability of the roundtrip frequency is observed by using QD gain material instead of bulk gain material.

The laser with a 540-μm SA section has lasing threshold current values of 830–910 mA for SA reverse bias voltages of −0.5 to −2.5 V, respectively. This increase of the threshold current as compared to the 270 μm laser is caused by the increased SA length and the correspondingly increased absorption in the laser cavity. The RF spectra obtained for this laser show that mode-locking only sets in at relatively high values of the injection current, i.e., around 1.0 A. For the SA bias voltages of −2.0 down to −2.5 V, mode-locking sets in close to 1.2 A. This is the upper limit for our measurement setup, since above this value of the injection current, the detrimental effect of device heating causes the output power to drop. The output power in this regime of stable mode-locking is between 1– 4 mW. Comparing the results obtained with the 270 and the 540 μm SA, it seems that the effect of an increased voltage on the SA and an increased length of the SA are interchangeable with respect to the stability of mode-locking.

For comparison we studied the 9-mm one-section laser. The threshold current of this device is 380 mA. The electrical spectrum shows no distinct peak at the roundtrip frequency. This can be expected based on the well-known mechanisms of passive mode-locking in laser diodes with bulk or quantum-well gain material, where the SA plays a crucial role [1], [8]. However, one-section quantum-dash and QD FP-lasers emitting around 1.55 μm have been reported to show passive mode-locking, without the aid of an SA [15], [16].

Timing jitter has been studied by evaluating the single-sideband phase noise signal around the fundamental RF peak, using an integration interval of 10 kHz–80 MHz. In Fig. 4, it can be seen that next to the dc component of the spectrum (i.e., the low-frequency components), no pedestal is observed above the noise floor of the analyzer, so the contribution of the amplitude jitter can be neglected in this evaluation [26]. The timing jitter has been evaluated for the 270-μm SA device at a fixed injection current of 900 mA. The value is (35 ± 3) ps for a low SA bias voltage of −0.5 V and increases slightly to (39 ± 3) ps for an SA bias voltage of −2 V. For the 540-μm SA device (evaluated at 1100 mA), this increase of the timing jitter is larger, going from (36 ± 4) ps to (53 ± 7) ps for SA bias voltages of −0.5 and −2 V, respectively. We note that the mode-locking in the 540 μm device is significantly less robust, as can be seen in Fig. 3.

The low-observed dc-pedestal (Fig. 4) is to be compared to typical bulk gain MLLD electrical spectra [25]. In these lasers clear signals are visible in the low frequency ranges <1 GHz of
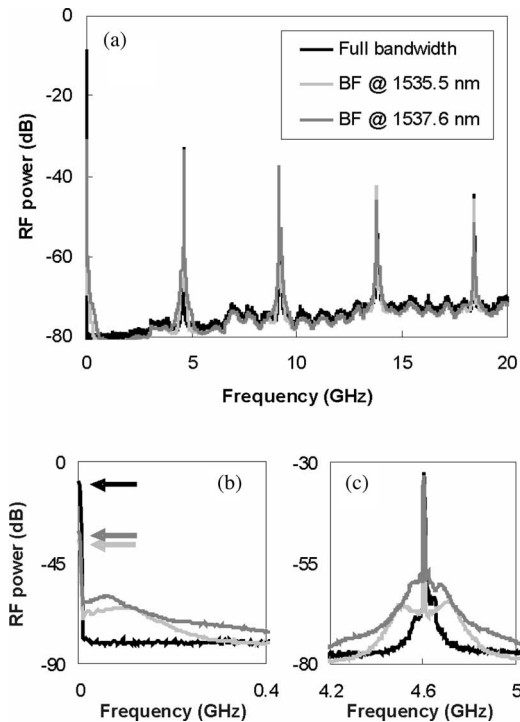
Fig. 4. (a) Electrical RF power spectra obtained at −1 V and 1.0 A injection current. The output with the full bandwidth (black) is compared to the output with the 0.22-nm bandpass filter placed at 1535.5 and 1537.6 nm. (b) The dc-peak and (c) the first RF peak are shown in detail. The arrows in (b) indicate the maxima of the dc-peaks.
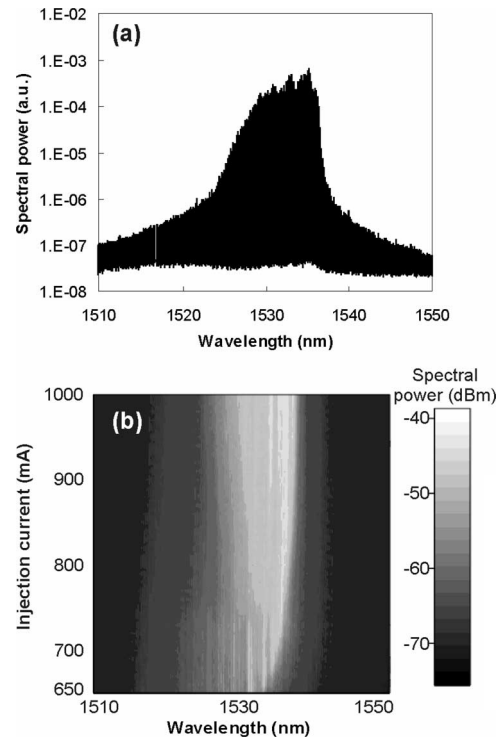

Fig. 5. (a) Optical spectrum obtained from the 270 μm SA device. The injection current is 900 mA and SA bias voltage is −1 V. The optical bandwidth used to obtain the spectrum is 0.16 pm. (b) Evolution of the optical spectrum for SOA injection currents varying from 650 mA up to 1.0 A. The SA bias voltage is −1 V. The spectral power is grayscale coded in dB.

at least 15 dB above the noise floor and at most 33 dB below the peak at the fundamental frequency. However, if we filter the QD laser output with a 0.22-nm bandpass filter, a significant increase of the pedestal at the low-frequency components can be seen. With this bandpass filter an increased pedestal is also observed around the RF peaks (see Fig. 4). The dc-pedestal corresponds to an amplitude jitter component, [26] and it can be concluded that power exchange between the different spectral components takes place. Comparing the facts that the MLLD output has a relatively large timing jitter and a low dc-pedestal, we conclude that the total jitter of the full-bandwidth output is dominated by phase jitter, largely owing to the power exchange between the different spectral components of the output.

As reported previously [19] using a 6-GHz real-time oscilloscope, a pulse train with a large dc-offset, or background, was observed from a photodiode recording the full optical laser output. Filtering of the output by a bandpass filter resulted in pulses with a strongly decreased background and a higher modulation depth. These previous results are confirmed by the signals from the RF analyzer, where a decrease in the dc-component relative to the harmonics in the electrical spectrum is observed when the bandpass filter is added (Fig. 4).

A typical optical spectrum of a 9-mm two-section laser is given in Fig. 5(a). The evolution of the optical spectrum as a function of the SOA injection current is presented in Fig. 5(b) for an SA bias voltage of −1 V. The spectrum is broad, i.e., 6–7 nm, as can be expected from the inhomogeneously broad-

ened gain of QD lasers [18]. Note that the spectra have a similar shape for all current values. The largest intensity is always on the long wavelength side of the spectrum and the intensity tails off in the direction of the shorter wavelengths.

Over the whole range of stable mode-locking no pulse is observed on the autocorrelator. However, when a 1.2-nm optical bandpass filter is added to the output of the laser, background-free pulses can be observed with the autocorrelator, with a duration of 6–11 ps [19]. With a real-time 6 GHz oscilloscope and with the bandpass filter pulses are observed with a modulation down to the 0 V level and over the full bandwidth, as can be seen in Fig. 6(b).

To investigate the timing between these separate spectral components of the output pulse, the setup of Fig. 6(a) is used [19]. Here, the output pulses of the laser are split using a 3 dB coupler and they are separately filtered using two optical bandpass filters (with bandwidths of 1.2 and 2.0 nm, respectively). Both filtered output pulses are then recorded with the 6 GHz oscilloscope. One of the bandpass filters (with 2.0 nm bandwidth) is kept at a fixed position and is used to trigger the signal, i.e., it serves as a reference. The other bandpass filter (with 1.2 nm bandwidth) is tuned and the output is recorded by the oscilloscope with the reference signal as a trigger. The oscilloscope traces are shown in Fig. 6(b). Using these oscilloscope traces the relative delay of the pulse trains resulting after filtering is then determined. This leads to the conclusion that the output pulse of the QD laser
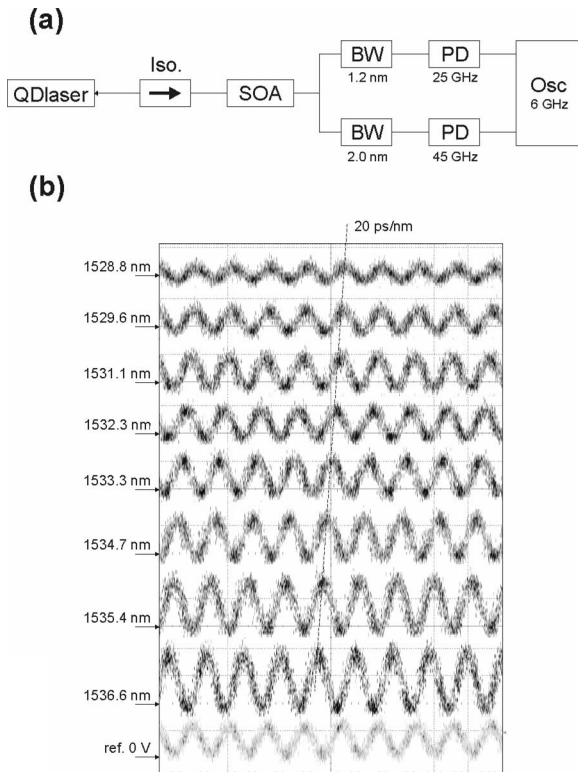
(a)

(b)

Fig. 6. (a) Schematic of the setup used to investigate the timing of the spectral components of the pulse. The two photodiodes (PDs) are connected to two channels of the oscilloscope (Osc). (b) A typical example of the oscilloscope traces. The signal at the indicated wavelengths is obtained with the 1.2 nm filter and the "ref." with the 2.0 nm filter. The traces have been vertically offset for easy comparison, with the arrows indicating the 0–V level.

Fig. 7. Autocorrelator traces (second harmonic power given) obtained from a 270-μm SA device. The injection current is 900 mA and the SA bias voltage is -1 V. The length of SMF between the device and the autocorrelator is indicated. An external SOA, placed before the SMF, is used for amplification.

is very elongated and heavily up-chirped, with a chirp value of about 20 ps/nm [19].

This observation of elongated, chirped pulses can be confirmed by studying compression of the pulses, using standard single-mode optical fiber (SMF). This technique has been used in [27] to convert the output of FM-locked lasers to a pulse train. The second-order dispersion of the SMF is on the order of 16–20 ps/(nm · km), so that 1.0–1.2 km of SMF should be able to compensate the chirp of these pulses. In Fig. 7, the autocorrelator traces are shown of the 270-μm SA laser output after passing through different lengths of SMF. As can be seen, the pulse is compressed to a minimum duration of the second harmonic generated signal with 1500 m of SMF. This minimum duration is 20–25 ps. However, the strong peaks in the center (for all shown fiber lengths) indicate a nonideal partial compression. This partial compression is probably caused by a nonlinear part of the chirp (or higher order SMF dispersion). Note that it is not possible to obtain autocorrelator traces without SMF, since the peak power of the elongated pulses is too low and the duration is too long (the pulses even overlap in time) [19]. We also note that the central, narrow peaks in the autocorrelator traces appear as a result of the dispersion of the SMF. This indicates that these peaks are not coherence spikes. The width of the narrow peaks decreases from 5 to 1 ps when the length of the SMF is increased from 800 to 1500 m.
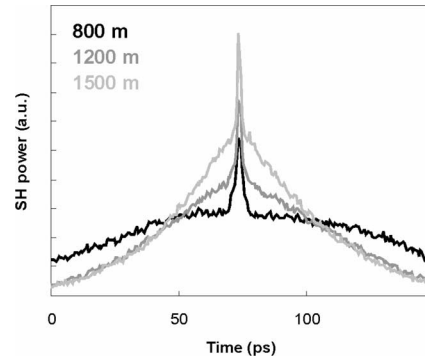
B. Effect of ES Lasing in 4 mm MLLDs

In this paragraph, we compare the results obtained with 4 mm MLLDs having a 120 and a 240 μm SA. Again a single-section 4-mm FP-laser, fabricated on the same chip, is used for reference purposes. The laser with a 120-μm SA section has lasing threshold current values from 330 to 410 mA for SA reverse bias voltages from 0 to -8 V, respectively. The laser with the longer 240 μm SA has threshold current values of 455–505 mA for bias voltages of 0 down to -2 V. The reference, single-section laser has a threshold value of 160 mA. Since these lasers are significantly shorter than those discussed in the previous section, the question is how the operation of these lasers is affected by the approximately 1.5–2 times higher current densities in the optical amplifier. As will be shown, the consequence is that the excited states in the quantum dots start playing a role.

The mapping of the RF-peak height of the lasers with 120 and 240 μm SAs is shown in Fig. 8. For the 120 μm laser, there is only a small area where stable mode-locking takes place. Between 600 and 750 mA SOAs injection current and between 0 and -2 V SAs bias voltage the RF peaks are over 40 dB above the noise floor. Optical output powers in this range are 3–5 mW. For the 240-μm SA laser, there are two areas in this mapping where stable mode-locking takes place, i.e., around 0 V and around the higher injection currents of 700–800 mA, respectively. The optical output powers at stable locking are 3–4 mW at the gain-section side of the laser. The shape of these areas is unlike the 9 mm device results, where there was only one large area of stability (see Fig. 3). To investigate this further, we first have a look at the optical spectra.

The optical output spectra of these 4 mm MLLDs are characterized by two main features at higher SOA injection currents, as can be seen in Fig. 9. With increasing injection current a group of modes appears at the shorter wavelength side, next to the main group of modes. Eventually, by increasing the current even further, this group seems to merge into the main group of modes. This is quite unlike what we observe with the 9 mm lasers. Since this double structured spectrum is also observed in our test FP lasers and in [18], [23], we ascribe this effect to the ES lasing and not to particular dynamics of the mode-locking
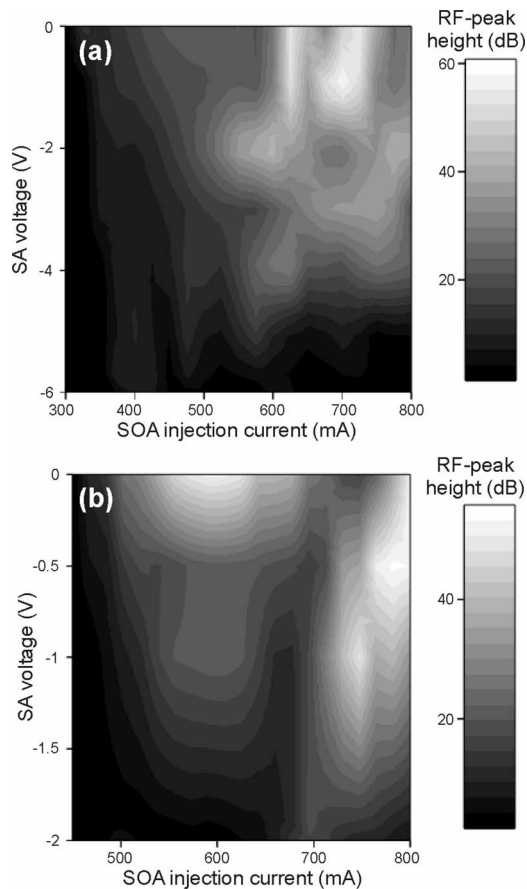
Fig. 8. Peak height in the RF power spectra (over the noise floor, dB-scale) for a 4 mm laser with (a) a 120 μm SA and (b) a 240 μm SA. The electrical bandwidth used to obtain the RF spectra is 50 kHz. An external SOA was used before the 50 GHz photodiode to boost the optical output power of the laser.

Fig. 9. Optical spectra (grayscale coded in dB), height of the first RF peak (black, lower axis), and width of the first RF peak at −20 dB of the maximum (gray, upper axis) as a function of the SOA injection current for (a) a 4 mm MLLD with a 120 μm SA, biased at −1 V and (b) a 4 mm MLLD with a 240 μm SA, biased at 0 V.

mechanism [28], [29]. This has been verified as described near the end of this section.

To investigate the effect of the appearance of this group of modes on the stability of mode-locking, the RF spectra are studied again. In Fig. 9, we have plotted the RF-peak height and the RF linewidth at −20 dB of the peak next to the optical spectra. As can be seen for both the 120 and 240-μm SA lasers the RF-peak height decreases with increasing power in the second group of modes. When this group merges into the primary group of modes, the RF-peak height increases again (black line in Fig. 9). When the lasers mode-lock, one can see the RF linewidth (gray line in Fig. 9) decreasing with increasing RF-peak height, down to values of 1.1 MHz for the 120 μm SA laser and 2.7 MHz for the 240 μm SA laser around 600 mA. A second regime of stable mode-locking in the 240 μm SA laser starts around 800 mA, with an RF linewidth of 1.6 MHz.

This leads to the conclusion that the appearance of optical gain in a separate wavelength region allows for the appearance of the second group of modes in the optical spectrum. This seems to destabilize the mode-locking in the 4 mm devices. The appearance of the second region in the gain spectrum allows for richer dynamics, which is, however, detrimental for stable mode-locking.
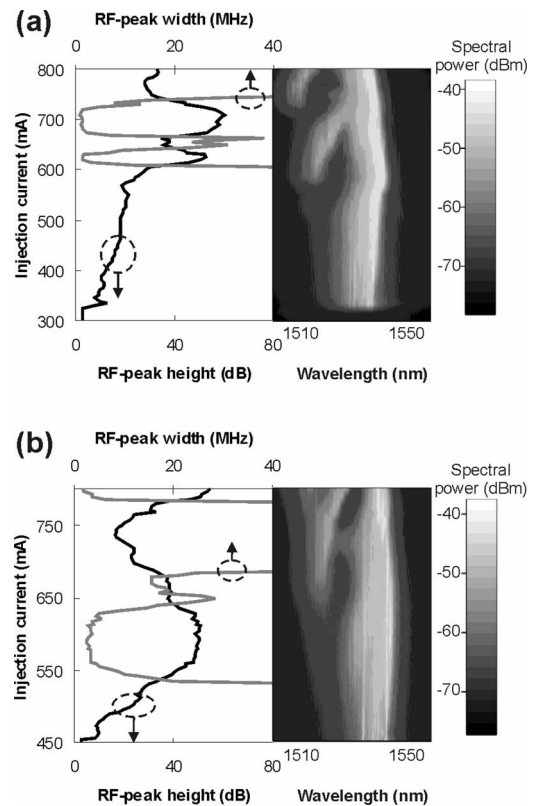
To study this second, shorter wavelength group of modes more closely, the setup of Fig. 10(a) is used. This setup is based on the same technique we used in [19] to obtain the chirp profile of the output pulses of the 9 mm MLLD. This chirp has a value of approximately 20 ps/nm as mentioned above. For the measurements on the 4 mm devices, we used a 13-GHz bandwidth real-time oscilloscope that can digitize at 40 Gigasamples per second (LeCroy SDA 13 000). With this oscilloscope, it is possible to record the individual pulses from the 10 GHz lasers in real time. The 4 mm MLLD with a 120 μm SA is evaluated at an SA bias voltage of −1 V and an SOA injection current of 630 mA. At these settings, an optical spectrum with two clear maxima is observed [Fig. 9(a)].

First the relative timing of the different spectral components is studied. The output pulses of the laser are split using a 3 dB coupler, and they are separately filtered using two optical bandpass filters (with bandwidths of 1.2 and 2.0 nm, respectively). Both filtered output signals are then recorded with the 13 GHz oscilloscope. One of the bandpass filters (with 2.0 nm bandwidth) is kept at a fixed wavelength [position 0 in Fig. 10(b)] and is used as a reference. The other bandpass filter (with 1.2 nm bandwidth) is tuned in wavelength and the output of both signals is recorded by the oscilloscope in a 20-μs-long trace. The phase difference between the swept signal and the reference signal is then calculated. This phase difference is also plotted
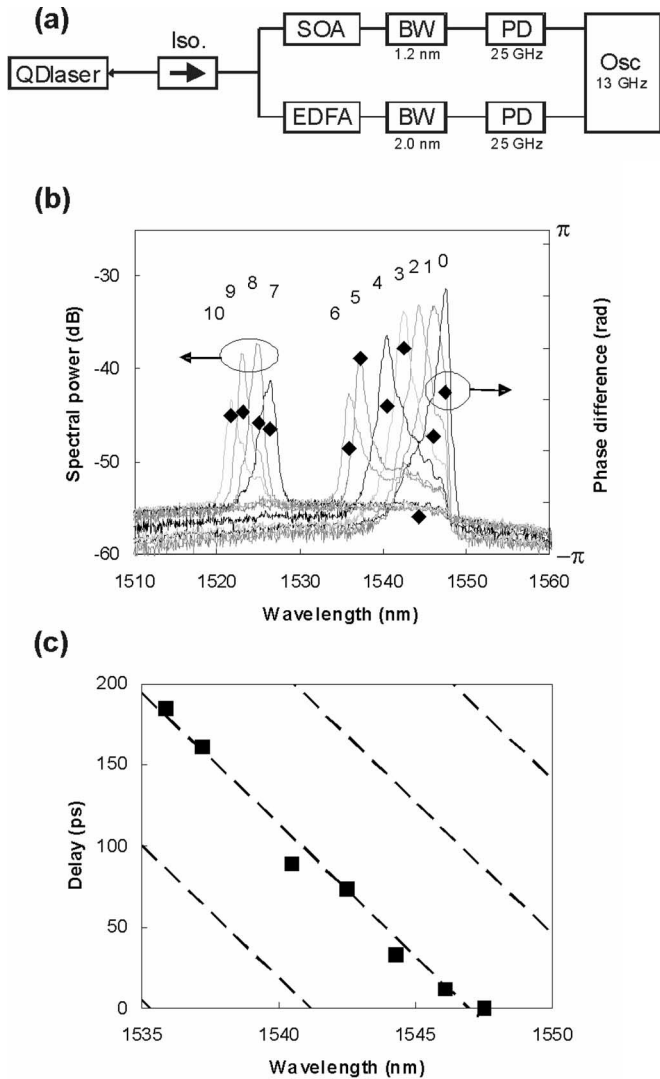
Fig. 10. (a) Schematic overview of the setup used to characterize the chirp of the QD lasers. PD: 25 GHz photodiode, BW: optical bandpass filter, Iso: optical isolator, SOA: semiconductor optical amplifier, EDFA: erbium-doped fiber amplifier, Osc: 13-GHz real-time oscilloscope. All equipment is fiber pigtailed or has fiber input or output connectors. (b) Power spectra of the light transmitted through the 1.2-nm optical bandpass filter at the ten positions used in the relative phase measurements and the measured relative phases of the pulses at each position of the filter. The phases are indicated by the diamonds and given relative to the "position 0" pulse. The presented data were taken from the 120-μm SA MLLD at an injection current of 630 mA and a bias voltage of -1 V. (c) Calculated delay for the different spectral components (squares), assuming a 10.5-GHz roundtrip frequency. The linear fit (dashed line) has a slope of 16 ps/nm. Multiple dashed lines show the periodicity of the laser.

in Fig. 10(b). It can be seen that the way the relative phase of the pulses changes over the wavelength regions in the output spectrum of the laser is strikingly different for the two groups of modes.

In the longer wavelength group the phase difference is decreasing with decreasing wavelength, assuming the smallest possible phase shifts (i.e., not taking multiples of 2π radians into account). This means that with decreasing wavelength the time delay between the signal at that wavelength and the reference signal increases. This increase of the time delay can be
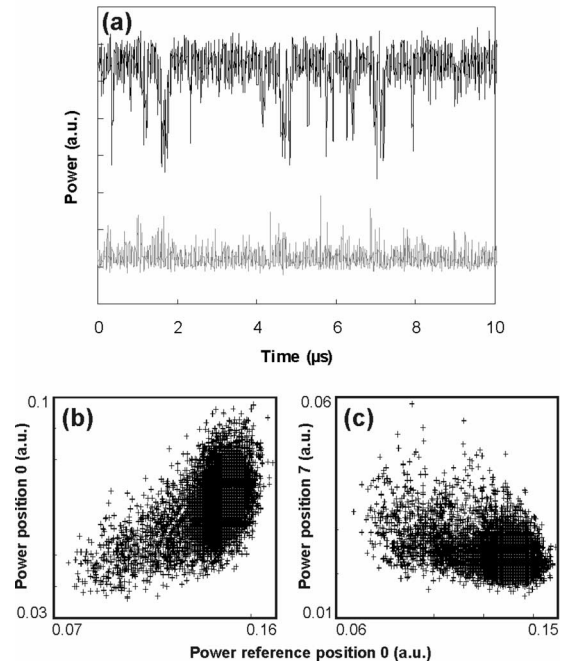

Fig. 11. (a) Time traces recorded with the oscilloscope, averaged more than 2.5 ns, showing signals at position 0 (black) and at position 7 (gray) (see Fig. 10). The setup of Fig. 10 is used. In (b,c) the reference signal is plotted against the signal at (b) position 0 and (c) position 7, taking the offset due to the nonequal optical and electrical signal path lengths into account.

expressed in time, since 2π radians correspond to the 95-ps roundtrip time for the 10.5 GHz laser, as shown in Fig. 10(c). The conclusion is that the pulses are predominantly linearly up-chirped with a value of approximately 16 ps/nm, close to the value of 20 ps/nm found for the 9 mm MLLDs. This means that the pulses are so elongated that they overlap inside the cavity.

The second group of modes (at the shorter wavelength side) seems to have no measurable delay between its spectral components. The reduced phase (i.e., ignoring multiples of 2π radians) is approximately equal to the phase of the right-hand-side components of the major group of modes [i.e., positions 1 and 2 in Fig. 10(b)]. Therefore, this group forms a pulse with limited or no chirp and fully synchronized with the pulse from the main group.

With the same setup, it is also possible to study intensity fluctuations in the laser output. To this end, we use the same two oscilloscope traces of signals at two wavelength bands and take the average signal power over every 2.5 ns of the 20 μs trace. A typical result with the traces from filter position 0 and at position 7 (see Fig. 10) is shown in Fig. 11. It can be observed that the power fluctuations at the two wavelengths show an anticorrelation. A dip in the power at filter position 0 corresponds with a peak in the power at filter position 7, with an offset. To get a more quantitative result, the power of the reference trace at position 0 is plotted versus the other traces at positions 0–10. The offset, which is an artifact of the setup, is minimized. Typical datasets appear as shown in Fig. 11. The correlation is then calculated (Pearson's r) and a maximum positive correlation is found at position 0. This can be understood since this is the same

position of the reference trace. A maximum negative correlation is found between position 7 and the reference trace. The fact that the right-hand sides of both groups of modes have the strongest correlation leads us to believe that the shorter wavelength group is due to ES lasing, and not an artifact of the inhomogeneous broadening [30]. The negative correlation is thus interpreted by us as a power exchange between the ground (GS) and ES lasing. After all, the most logical explanation for this maximum correlation to bridge about 20 nm in the spectrum would be that these wavelengths make use of the same set of dots, both at the GS and ES simultaneously. Spectral hole burning due to inhomogeneous broadening cannot account for this effect.

In summary, the analysis of the 4 mm MLLDs shows that the stability of the mode-locking is limited by the appearance of a second group of modes to the shorter wavelength side. Our observations in this paper confirm previous work [18], [23] that this is ES lasing, since we have observed a maximum power exchange between the longer wavelength spectral components of both groups, indicating that these spectral components should be coupled. This observation rules out the strong spectral hole burning due to the inhomogeneous broadening as a cause [30].

Apparently, increasing the SOA injection current in the 4 mm MLLDs can suppress this ES lasing and results in a more stable mode-locking performance. We explain this by assuming that with increased injection current the optical bandwidth of the GS group of modes is increased at the expense of the ES group of modes. We note that high-reflection coating of (one of) the chip facets will lead to lower current densities for the 4 mm lasers. As a consequence, ES lasing is not occurring, which could lead to more stable mode-locking.

IV. CONCLUSION

In this paper, we have shown that QD-based MLLDs operating around wavelengths of 1.55 μm can have a large and stable operating regime. In 9-mm, 4.6-GHz devices, we have found stable mode-locking with RF peaks of more than 40 dB for SOA injection currents between 750 mA and 1.0 A and for SA bias voltages of 0 V down to -3 V. The variation in the roundtrip frequency over this range is less than 6 MHz. Having such a large, stable operating regime is essential for practical implementation of these devices, since they are tolerant against variations in operating parameters. This operating regime is larger than the regime that is typically found in bulk or quantum-well MLLDs, operating around 1.55 μm, where typically the absorber voltage has to be decreased for increasing injection current [24], [25], and [31].

The timing jitter values for the 9 mm MLLDs are relatively large at 30–40 ps. We think that the main cause for this jitter is the power exchange between different spectral components of the laser output, resulting in a phase jitter of the output pulses. However, the presence of an SA in these devices may possibly allow for hybrid mode-locking. This technique can in principle severely decrease the timing jitter. Since the pulses are very elongated, hybrid mode-locking will probably alter the mode-locking dynamics significantly.

Analysis of the shorter 4 mm MLLDs shows that the regime of stable mode-locking is mainly limited by the appearance of the ES lasing with increasing SOA current. However, it appears that these modes can be suppressed when this injection current is increased even further, resulting in stable islands in the operating regime.

The output spectrum of these devices is shown to be coherent and has a broad bandwidth of 6–7 nm. However, the output pulses are highly chirped and very elongated. These chirped pulses have a duration on the order of the roundtrip time for the 9 mm MLLDs, but in the 4 mm MLLDs, these pulses overlap inside the cavity. Although the mechanism of mode-locking in these novel QD devices is not fully understood yet, we note that the SA plays an essential role, much unlike previously reported QD lasers operating at the same wavelengths [15], [28]. We ascribe the elongated, chirped output pulses to the relatively small homogeneous broadening of the gain and absorption in these devices and the related spectral hole burning. We think that a modeling approach that takes these effects into account [29], [30] will be necessary for further investigation of the dynamics in these QD lasers.

These MLLDs have been realized with a fabrication technology that is compatible with further photonic integration [22], [23]. As such these devices can perform the function of, e.g., a coherent multiwavelength source or even a mode-comb generator in a complex photonic chip.

ACKNOWLEDGMENT

REFERENCES

[1] R. Kaiser and B. Hüttl, "Monolithic 40-GHz mode-locked MQW DBR lasers for high-speed optical communication systems," *IEEE J. Sel. Topics Quantum Electron.*, vol. 13, no. 1, pp. 125–135, Jan./Feb. 2007.

[2] R. G. Broeke, J. Cao, C. Ji, S.-W. Seo, Y. Du, N. K. Fontaine, J.-H. Baek, J. Yan, F. M. Soares, F. Olsson, S. Lourdudoss, A.-V. H. Pham, M. Shearn, A. Scherer, and S. J. B. Yoo, "Optical-CDMA in InP," *IEEE J. Sel. Topics Quantum Electron.*, vol. 13, no. 5, pp. 1497–1507, Sep./Oct. 2007.

[3] N. K. Fontaine, R. P. Scott, J. Cao, A. Karalar, W. Jiang, K. Okamoto, J. P. Heritage, B. H. Kolner, and S. J. B. Yoo, "32 phase × 32 amplitude optical arbitrary waveform generation," *Opt. Lett.*, vol. 32, no. 7, pp. 865–867, Apr. 2007.

[4] B. Jalali and S. Fathpour, "Silicon Photonics," *J. Lightw. Technol.*, vol. 24, no. 12, pp. 4600–4615, Dec. 2006.

[5] B. R. Koch, A. W. Fang, O. Cohen, and J. E. Bowers, "Mode-locked silicon evanescent lasers," *Opt. Exp.*, vol. 15, pp. 11225–11233, 2007.

[6] H. Guo, K. Sato, K. Takashima, and H. Yokoyama, "Two-photon bio-imaging with a mode-locked semiconductor laser," presented at the 15th Int. Conf. Ultrafast Phenomena, Pacific Grove, CA, Aug. 2006, Paper TuE8.

[7] K. W. Holman, D. J. Jones, J. Ye, and E. P. Ippen, "Orthogonal control of the frequency comb dynamics of a mode-locked laser diode," *Opt. Lett.*, vol. 28, no. 23, pp. 2405–2407, Dec. 2003.

[8] K. A. Williams, M. G. Thompson, and I. H. White, "Long-wavelength monolithic mode-locked diode lasers," *New J. Phys.*, vol. 6, pp. 179-1–179-30, Nov. 2004.

[9] E. U. Rafailov, M. A. Cataluna, and W. Sibbett, "Mode-locked quantum-dot lasers," *Nat. Photon.*, vol. 1, pp. 395–401, Jul. 2007.

[10] D. Bimberg, M. Grundmann, F. Heinrichsdorff, N. N. Ledentsov, V. M. Ustinov, A. E. Zhukov, A. R. Kovsh, M. V. Maximov, Y. M. Shernyakov, B. V. Volovik, A. F. Tsatsul'nikov, P. S. Kop'ev, and

Zh. I. Alferov, "Quantum dot lasers: Breakthrough in optoelectronics," *Thin Solid Films*, vol. 367, no. 1–2, pp. 235–249, May 2000.

[11] M. G. Thompson, A. Rae, R. L. Sellin, C. Marinelli, R. V. Penty, I. H. White, A. R. Kovsh, S. S. Mikhrin, D. A. Livshits, and I. L. Krestnikov, "Subpicosecond high-power mode locking using flared waveguide monolithic quantum-dot lasers," *Appl. Phys. Lett.*, vol. 88, pp. 133119-1–133119-3, 2006.

[12] E. U. Rafailov, M. A. Cataluna, W. Sibbett, N. D. Il'inskaya, Y. M. Zadiranov, A. E. Zhukov, V. M. Ustinov, D. A. Livshits, A. R. Kovsh, and N. N. Ledentsov, "High-power picosecond and femtosecond pulse generation from a two-section mode-locked quantum-dot laser," *Appl. Phys. Lett.*, vol. 87, pp. 081107-1–081107-3, 2005.

[13] M. Kuntz, G. Fiol, M. Lammlin, D. Bimberg, M. G. Thompson, K. T. Tan, C. Marinelli, R. V. Penty, I. H. White, V. M. Ustinov, A. E. Zhukov, Yu. M. Shernyakov, and A. R. Kovsh, "35 GHz mode-locking of 1.3 μm quantum dot lasers," *Appl. Phys. Lett.*, vol. 85, pp. 843–845, 2004.

[14] Y. Barbarin, S. Anantathanasarn, E. A. J. M. Bente, Y.-S. Oei, M. K. Smit, and R. Nötzel, "1.55-μm range InAs-InP (100) quantum-dot Fabry-Pérot and ring lasers using narrow deeply etched ridge waveguides," *IEEE Photon. Technol. Lett.*, vol. 18, no. 24, pp. 2644–2646, Dec. 2006.

[15] C. Gosset, K. Merghem, A. Martinez, G. Moreau, G. Patriarche, G. Aubin, A. Ramdane, J. Landreau, and F. Lelarge, "Subpicosecond pulse generation at 134 GHz using a quantum-dash-based Fabry-Perot laser emitting at 1.56 μm," *Appl. Phys. Lett.*, vol. 88, pp. 241105-1–241105-3, 2006.

[16] Z. G. Lu, J. R. Liu, S. Raymond, P. J. Poole, P. J. Barrios, and D. Poitras, "312-fs pulse generation from a passive C-band InAs/InP quantum dot mode-locked laser," *Opt. Exp.*, vol. 16, no. 14, pp. 10835–10840, Jul. 2008.

[17] F. Lelarge, B. Dagens, J. Renaudier, R. Brenot, A. Accard, F. van Dijk, D. Make, O. le Gouezigou, J.-G. Provost, F. Poingt, J. Landreau, O. Drisse, E. Derouin, B. Rousseau, F. Pommereau, and G.-H. Duan, "Recent advances on InAs/InP quantum dash based semiconductor lasers and optical amplifiers operating at 1.55 μm," *IEEE J. Sel. Topics Quantum Electron.*, vol. 13, no. 1, pp. 111–124, Jan./Feb. 2007.

[18] S. Anantathanasarn, R. Nötzel, P. J. van Veldhoven, F. W. M. van Otten, Y. Barbarin, G. Servanton, T. de Vries, E. Smalbrugge, E. J. Geluk, T. J. Eijkemans, E. A. J. M. Bente, Y.-S. Oei, M. K. Smit, and J. H. Wolter, "Lasing of wavelength-tunable (1.55 μm region) InAs/InGaAsP/InP (100) quantum dots grown by metal organic vapor-phase epitaxy," *Appl. Phys. Lett.*, vol. 89, pp. 073115-1–073115-3, Aug. 2006.

[19] M. J. R. Heck, E. A. J. M. Bente, E. Smalbrugge, Y.-S. Oei, M. K. Smit, S. Anantathanasarn, and R. Nötzel, "Observation of Q-switching and mode locking in two-section InAs/InP (100) quantum dot lasers around 1.55 μm," *Opt. Exp.*, vol. 15, no. 25, pp. 16292–16301, Dec. 2007.

[20] R. Huber, M. Wojtkowski, and J. G. Fujimoto, "Fourier domain mode locking (FDML): A new laser operating regime and applications for optical coherence tomography," *Opt. Exp.*, vol. 14, no. 8, pp. 3225–3237, Apr. 2006.

[21] J.-P. Tourrenc, M. T. Todaro, S. P. Hegarty, C. Kelleher, B. Corbett, G. Huyet, and J. G. McInerney, "High performance passively mode-locked 1.3 μm quantum-dot lasers," presented at the 15th Int. Conf. Ultrafast Phenomena, Pacific Grove, CA, 2006, Paper WC9.

[22] J. J. M. Binsma, M. van Geemert, F. Heinrichsdorff, T. van Dongen, R. G. Broeke, and M. K. Smit, "MOVPE waveguide regrowth in InGaAsP/InP with extremely low butt joint loss," in *Proc. Symp. IEEE/LEOS Benelux Ch.*, Brussels, Dec. 2001, pp. 245–248.

[23] H. Wang, J. Yuan, P. J. van Veldhoven, T. de Vries, B. Smalbrugge, E. J. Geluk, E. A. J. M. Bente, Y.-S. Oei, M. K. Smit, S. Anantathanasarn, and R. Nötzel, "Butt joint integrated extended cavity InAs/InP (100) quantum dot laser emitting around 1.55 μm," *Electron. Lett.*, vol. 44, no. 8, pp. 522–523, Apr. 2008.

[24] U. Bandelow, M. Radziunas, A. Vladimirov, B. Hüttl, and R. Kaiser, "40 GHz mode-locked semiconductor lasers: theory, simulations and experiment," *Opt. Quantum Electron.*, vol. 38, no. 4–6, pp. 495–512, Mar. 2006.

[25] Y. Barbarin, E. A. J. M. Bente, M. J. R. Heck, Y.-S. Oei, R. Nötzel, and M. K. Smit, "Characterization of a 15 GHz integrated bulk InGaAsP passively mode-locked ring laser at 1.53 μm," *Opt. Exp.*, vol. 14, no. 21, pp. 9716–9727, 2006.

[26] D. von der Linde, "Characterization of the noise in continuously operating mode-locked lasers," *Appl. Phys. B.*, vol. 39, pp. 201–217, 1986.

[27] S. R. Chinn and E. A. Swanson, "Passive FM locking and pulse generation from 980-nm strained-quantum-well Fabry-Perot lasers," *IEEE Photon. Technol. Lett.*, vol. 5, no. 9, pp. 969–971, Sep. 1993.

[28] J. Liu, Z. G. Lu, S. Raymond, P. J. Poole, P. J. Barrios, and D. Poitras, "Dual-wavelength 92.5 GHz self-mode-locked InP-based quantum dot laser," *Opt. Lett.*, vol. 33, no. 15, pp. 1702–1704, Aug. 2008.

[29] C. Xing and E. A. Avrutin, "Multimode spectra and active mode locking potential of quantum dot lasers," *J. Appl. Phys.*, vol. 97, pp. 104301-1–104301-9, 2005.

[30] M. Sugawara, K. Mukai, Y. Nakata, H. Ishikawa, and A. Sakamoto, "Effect of homogeneous broadening of optical gain on lasing spectra in self-assembled InxGa1-xAs/GaAs quantum dot lasers," *Phys. Rev. B*, vol. 61, no. 11, pp. 7595–7603, Mar. 2000.

[31] R. Kaiser, B. Huttl, H. Heidrich, S. Fidorra, W. Rehbein, H. Stolpe, R. Stenzel, W. Ebert, and G. Sahin, "Tunable monolithic mode-locked lasers on InP with low timing jitter," *IEEE Photon. Technol. Lett.*, vol. 15, no. 5, pp. 634–636, May 2003.

Martijn J. R. Heck (S'04–M'09) was born in Nijmegen, The Netherlands, in 1976. He received the M.Sc. degree in applied physics and the Ph.D. degree from Eindhoven University of Technology, Eindhoven, The Netherlands, in 2002 and 2008, respectively.

From 2007 to 2008, he has been a Postdoctoral Researcher at the Communication Technology: Basic Research and Applications (COBRA) Research Institute, Eindhoven University of Technology, Eindhoven, The Netherlands, where he was engaged in the development of a technology platform for active–passive integration of photonic integrated circuits. From 2008 to 2009, he was also with the Laser Centre Vrije Universiteit, Amsterdam, The Netherlands, where he was involved in the development of integrated frequency combs.

He is currently a Postdoctoral Researcher at the Department of Electrical Engineering, University of California Santa Barbara, where he works on photonic integrated circuits based on the heterogeneous integration of silicon photonics with III/V materials.

Amandine Renault was born near Paris, France. She studied physics at Paris University VII and Paris University XI, Paris, France. She received the M.Sc. degree in research physics, with an orientation in Optics from Paris University VII and Paris University XI, in 2002, and the Ph.D. degree in physics from the Ecole Polytechnique, Palaiseau Cedex, France, in 2006.

From 2006 to 2008, she was a Postdoctoral Researcher on high-precision metrology using frequency comb lasers and parametric amplification at the Laser Centre Vrije Universiteit, Amsterdam, The Netherlands. She is currently a Development Engineer at ASML, Veldhoven, The Netherlands.

Erwin A. J. M. Bente (M'01) received the M.Sc. degree in physics and the Ph.D. degree from Vrije Universiteit, Amsterdam, The Netherlands, in 1983 and 1989, respectively.

From 1988 to 1994, he was with Urenco Nederland B.V. and led a research group on laser isotope separation. From 1994 to 1996, he was a Researcher with Vrije Universiteit, where he worked on solid-state coherent light sources and isotope separation of stable isotopes. He worked as a Research Team Leader at the Institute of Photonics, University of Strathclyde, Glasgow, U.K., and was involved in high-power diode-pumped solid-state lasers, passive mode-locking, and femtosecond laser machining. Since 2001, he has been an Assistant Professor at the Communication Technology: Basic Research and Applications (COBRA) Research Institute, Eindhoven University of Technology, Eindhoven, The Netherlands, where he is involved in integrated semiconductor laser systems.

Dr. Bente is a member of the Institute of Physics and the Optical Society of America.

Yok-Siang Oei is an Associate Professor in the Department of Electrical Engineering, Eindhoven University of Technology, Eindhoven, The Netherlands, where he is within the Communication Technology: Basic Research and Applications (COBRA) Research Institute and is responsible for the development of the fabrication technology of InP-based devices. He is the author or coauthor of more than 150 journal and conference papers. His current research interests include the monolithic integration of photonic devices.

Meint K. Smit (F'03) received the M.Sc. degree (with honors) and the Ph.D. degree (with honors) in electrical engineering from Delft University of Technology, Delft, The Netherlands, in 1974 and 1991, respectively.

In 1974, he started work on radar and radar remote sensing. In 1976, he joined Delft University of Technology, where he became the Leader of the Photonic Integrated Circuits Group in 1994, and was appointed as a Professor in 1998. In 2002, he moved with the Photonic Integrated Circuits Group to Eindhoven University of Technology, Eindhoven, The Netherlands, where he is currently the Leader of the Optoelectronic Devices Group, Communication Technology: Basic Research and Applications (COBRA) Research Institute. In 1997, he received a research grant to establish the National Research Center on Photonics.

Dr. Smit became a Fellow of the IEEE Lasers and Electro-Optics Society in 2002 for contributions in the field of optoelectronic integration. He is the inventor of the arrayed waveguide grating, for which he received a Lasers and Electro-Optics Society (LEOS) Technical Award in 1997.

Kjeld S. E. Eikema received the M.Sc. and Ph.D. degrees in physics from Vrije Universiteit, Amsterdam, The Netherlands, in 1991 and 1996, respectively.

He is currently an Associate Professor at the Laser Centre Vrije Universiteit, Amsterdam, The Netherlands, where he started a group on ultrafast laser physics in 2000, after obtaining a NWO VIDI grant. From 1996 to 2000, he was a Postdoctoral Fellow at Max Planck Institute for Quantum Optics, Munich, Germany, where he worked on laser-cooling of antihydrogen . He received the European Physical Society (EPS) Fresnel prize 2003. In 2007, he received a NWO VICI grant for his research activities involving ultrafast phase-controlled pulses and applications of it in precision frequency metrology and attosecond science.

Wim Ubachs received the Ph.D. degree in physics from Nijmegen University, The Netherlands, in 1986.

He is currently a Professor of Atomic, Molecular and Laser Physics, Vrije Universiteit, Amsterdam, The Netherlands, where he is also a Director of the Laser Centre. In 1986, he was a Postdoctoral Fellow in Dalian, China and in Stanford University, CA, from 1987 to 1988. From 2001 to 2004, he held a part-time professorship at the Eindhoven University of Technology, Eindhoven, The Netherlands, guest professorship at the ETH Zürich in 2002, and at Tokyo University of Science, Tokyo, Japan, in 2006. His current research interests include laser development and the application of lasers in high-resolution spectroscopy, in particular the generation of tunable narrowband extreme ultraviolet radiation and its application to molecular spectroscopy. Recently he has become involved in metrology applications, such as the search for variation of fundamental constants.

Sanguan Anantathanasarn was born in Bangkok, Thailand, in 1976. He received the M.Eng. and Ph.D. degrees in electronics and information engineering from Hokkaido University, Sapporo, Japan, in 2000 and 2003, respectively.

From 2003 to 2004, he was a Research Fellow at the Japan Center of Excellence, Research Center for Integrated Quantum Electronics, Hokkaido University, where he was engaged in research on gallium-nitride-based electronic devices. Since 2004, he has been with the Photonics and Semiconductor Nanophysics Group, Communication Technology: Basic Research and Applications (COBRA) Research Institute, Eindhoven University of Technology, Eindhoven, The Netherlands. His current research interests include the epitaxial growth of III–V semiconductor nanostructures and their application in optical fiber telecommunication systems.

Dr. Anantathanasarn is a member of the Japan Society of Applied Physics and the IEEE Lasers and Electro-Optics Society.

Richard Nötzel received the Diploma in physics from the Technical University of Munich, Munich, Germany, in 1989, and the Doctoral degree in semiconductor physics from the University of Stuttgart, Stuttgart, Germany, in 1992.

During 1993, he was with Nippon Telegraph and Telephone (NTT) Corporation, Atsugi, Japan. During 1994, he was a Visiting Associate Professor, and later, a Visting Professor at Hokkaido University, Sapporo, Japan. In 1995, he was with Paul Drude Institute for Solid State Electronics, Berlin, Germany. Since 2000, he has been an Associate Professor at Eindhoven University of Technology, Eindhoven, The Netherlands, where he is currently with the Communication Technology: Basic Research and Applications (COBRA) Inter-University Research Institute on Communication Technology, Eindhoven University of Technology, Eindhoven, The Netherlands. His current research interests include direct synthesis of low-dimensional semiconductors and their electronic properties for applications in novel photonic devices, and integrated circuits.

Dr. Nötzel was the recipient of the Berlin-Brandenburg Academy Award for Science, NTT Opto-Electronics Laboratories Award, and Otto Hahn Medal of the Max-Planck Society.